Modelling Near-field Effects in VSP-based Q-estimation

Part 2: Modelling Results

Arnim B. Haase*
CREWES, University of Calgary
haaseab@ucalgary.ca
and
Robert R. Stewart
University of Houston

Summary

The complete spherical wavefield emanating from a P-wave point source surrounded by a homogeneous isotropic medium is computed with the aid of Weyl/Sommerfeld integrals. In a resulting synthetic VSP, we observe a near-field, a far-field and a 90° phase rotation between the two. Depth dependence of magnitude spectra in these two depth regions is distinctly different. Log magnitude spectra show a linear dependence on frequency in the far-field but not in depth regions where the near-field becomes significant. Near-field effects are one possible explanation for large positive and even negative Q-factors in the shallow section that may be estimated from VSP data when applying the spectral ratio method. A near-field compensation method for Q-estimation in homogeneous models reduces errors in Q-values except in the immediate vicinity of the source.

Introduction

A zero-offset synthetic VSP computed with the aid of Weyl/Sommerfeld integrals can be seen in Part 1 of this contribution. We note a trace-to-trace amplitude decay with increasing depth and also a phase rotation. These observations are considered to be time-domain evidence for a near-field that quickly disappears with increasing depth in comparison to the far-field. In Part 2 we investigate the frequency-domain representation of near-field versus far-field phenomena and their impact on spectral-ratio-method Q-estimation. Next we apply near-field compensation of VSP-spectra as suggested in Part 1 for the reduction of Q-estimation errors. Lastly, near-field Q-estimation errors are further reduced by the non-linear log-ratio fitting introduced in Part 1.

Modelling Results

VSP-receivers are normally placed in the borehole with a constant depth interval between them. In a real-world VSP these depth stations receive upgoing and downgoing wave fields. In our chosen homogeneous model environment there are no reflections but only the transmitted source wavelet. That is to say our model includes neither surface effects, nor geophone clamping problems, nor multiples, nor soil compaction. Zero-offset synthetic VSP traces are computed with Equation 2 of Part 1. The parameters for this earth model are

V_p = 2000 m/s, V_s = 879.88 m/s, ρ = 2400 kg/m^3 and Q_p = 100. The zero-phase (non-causal) Ormsby wavelet employed for these computations has the parameters 5/15-80\100 Hz.

What would be the near-field Q-estimation error for the spectral ratio method (SRM)? To answer this question we examine near-field and far-field magnitude spectra next. Plotted in Figure 1 are log-magnitude spectra, computed with the Sommerfeld-integral given in Equation 2 of Part 1, for the depth range of 15 m to 61 m. This is thought to be the depth range where the near-field term (decaying with $1/z^2$) dominates the far-field term (decaying with $1/z$). Global scaling to a maximum of zero dB is applied to the spectra in Figure 1; the relative amplitudes are retained. We note that attenuation increases with depth z and frequency ω. Nonlinear frequency dependence of log magnitude spectra in this depth region could be interpreted as a frequency dependent quality factor Q(ω), however the model computation uses constant Q. Relative scaling is lost when applying the spectral ratio method because multipliers become added constants on taking the logarithm; these added constants are part of the neglected intercept term. Figure 2 demonstrates what SRM "sees" (Haase and Stewart, 2007). The downgoing wave "*appears*" to gain high frequency strength: the shallower in depth the VSP-receiver station the steeper the slope of log magnitude spectra as a function of frequency, which implies negative Q-factors. Note that neither geophone coupling nor surface soil compaction are modelled here.

When computing log spectral ratios between depth levels 15 m and 38 m, we find a curve (Figure 3) which clearly is *not* a linear function of frequency. Fitting straight lines in three different frequency ranges leads to three different (negative) Q-estimates. It was noted above that log-magnitude spectra plotted in Figure 1 have increased slope angles with decreased depth. Close inspection of the deepest receiver (at 60.9 m depth) above approximately 50 Hz shows a trend change because far-field conditions are approached. Q-estimation leads to negative Q-factors near the source and large positive Q some distance away in the near-field where the slope trend is reversed but the log-magnitude curves are still almost parallel. As far-field conditions are approached the estimated Q converges with the model Q of 100. Q versus depth estimated in two different frequency bands is depicted in Figure 4. Note the "*wrap-around*" look at the depths where Q changes polarity.

Figure 5 (Haase and Stewart, 2007) gives log-magnitude spectra for the depth region of 61 m to 1113 m which is below that displayed in Figure 1, again computed with Equation 2 of Part 1. This is the far-field dominated depth region where Q-factor recovery is expected to be almost perfect because spectral ratio methods are derived for these circumstances with linear log ratio slopes. The deeper the receiver, the steeper the log-magnitude curve. Figure 6 compares SRM-derived $Q(z)$ to the model Q of 100. Note that negative Q-factors are not plotted in this diagram.

Where does the near-field stop and the far-field begin? Aki and Richards (1980) use the term "*many wavelengths*" when describing the distance from source points to where far-field approximations start to be accurate. Common practice is to assume that *several wavelengths* are sufficient for far-field approximation accuracy (E. Krebes, 2007, personal communication). From Equation 4 of Part 1 it is clear that near-fields diminish with increasing depth z and increasing frequency ω relative to the far-field. The term $V_p/(\omega z)$ in Equation 4 of Part 1 is proportional to λ/z where λ is the wave length. In Figure 7, λ/z is plotted as a function of z and ω. The maximum value of 1.0 represents the case of $\lambda=z$ and the minimum of 0.1 stands for $z=10\lambda$. At 10 Hz, the 10 % threshold is as deep as z=2000 m; in the other extreme at z=200 m the frequency must be increased to 100 Hz in order to reach the same 10% threshold. If we take the "*many wavelengths*" to mean 10λ then this prescribes a minimum evaluation frequency of 40 Hz for a depth of 500 m. "*Near-field*" and "*near-surface*" may not be strictly interchangeable.

Near-field Compensation of Q-estimates

In Part 1 we observed that all amplitudes are multiplied by a factor of $(1+iV_p/\omega z)$ and that in the far-field, where the depth z is large, and/or at higher frequencies ω, this multiplier approaches unity. As a first step towards near-field compensation we suggested to precondition the input spectra prior to Q-estimation

through division by this factor. Plotted in Figure 8 are spectra compensated for magnitudes of the above multiplier because the spectral ratio method operates on amplitudes and ignores phase information. When comparing to Figure 1 we note that, firstly, the near-field compensated spectra are much less curved and, secondly, their slopes increase with depth. The second point constitutes a complete reversal of the near-field *behaviour* observed in Figure 1. The steady increase of compensated spectral slopes with depth now precludes negative Q-factors. However, close inspection of Figure 8 reveals that spectral slopes "*move*" further apart with decreasing depths. This slope diversion and also any remnant curvature are expected to cause Q-estimation errors. Figure 6 shows that simple near-field compensation of amplitude spectra does improve Q-estimates to a certain extent. There are no negative Q-values in the new Q-estimate but at very shallow depths (above approximately 100 m) the quality factor is grossly underestimated.

Because the near-field multiplier given by Equation 4 in Part 1 is frequency dependent, a more accurate approach to near-field Q-estimation involves non-linear curve fitting of log-spectral-ratios (a curved near-field log-spectral-ratio is given in Figure 3). This is in contrast to the straight line fitting applied above and also displayed in Figure 3. The result of non-linear curve fitting using Equation 5 of Part 1 is plotted in Figure 6 and can be seen to extend the useful near-field Q-estimation range even closer to the source point.

Conclusions

The near-field of a P-wave point source decays faster with distance from the source than the far-field ($1/z^2$ versus $1/z$). It also decays with frequency. Because of the more rapid decay of low frequencies close to the source there is a "*relative*" increase in strength of high frequencies in this region leading to negative Q-estimates when the spectral ratio method is applied here. At some distance from the source, where log magnitude curves are parallel, the estimated Q would be infinite. Just beyond that (further away from the source point) Q-estimates show large positive values which will decrease towards the model-Q as the source-to-receiver distance is further increased and far-field conditions are approached. Near-field Q-estimates can be improved by near-field compensation which extends the useful Q-estimation range closer to the source point.

Acknowledgements

Support from the CREWES Project at the University of Calgary and its industrial sponsorship is gratefully acknowledged.

References

Aki, K.T., and Richards, P.G., 1980, Quantitative Seismology: Theory and Methods: Vol. 1, W.H. Freeman and Co.

Haase, A.B., and Stewart, R.R., 2007, Testing VSP-based Q-estimation with spherical wave models: CREWES Research Report, Volume 19.

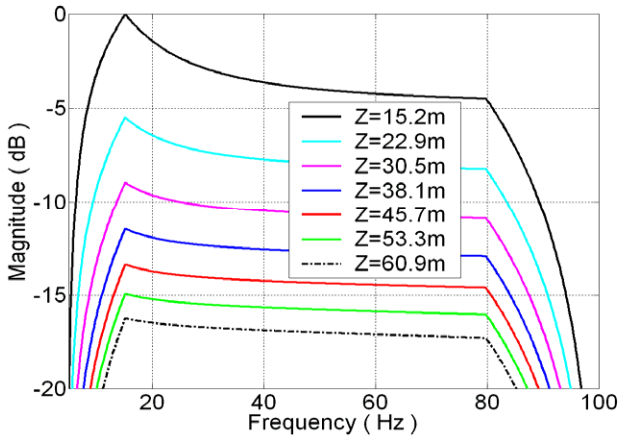

Figure 1: Near-field log-magnitude spectra (global scaling).

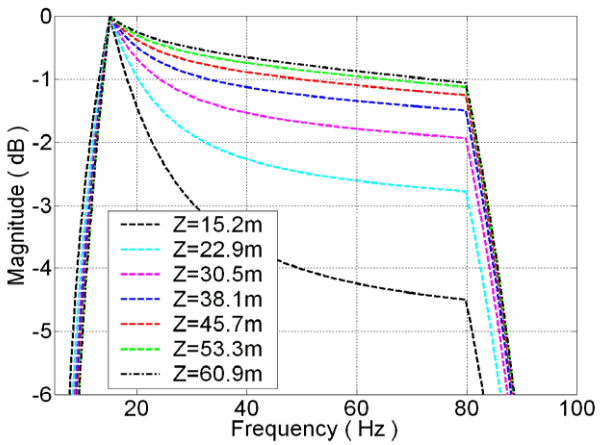

Figure 2: Spectra of Fig.1 equalized to their maximum amplitudes.

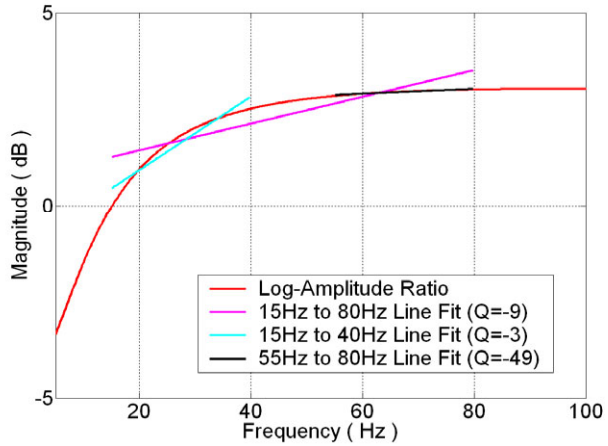

Figure 3: Straight line fit to log spectral ratio (38m/15m).

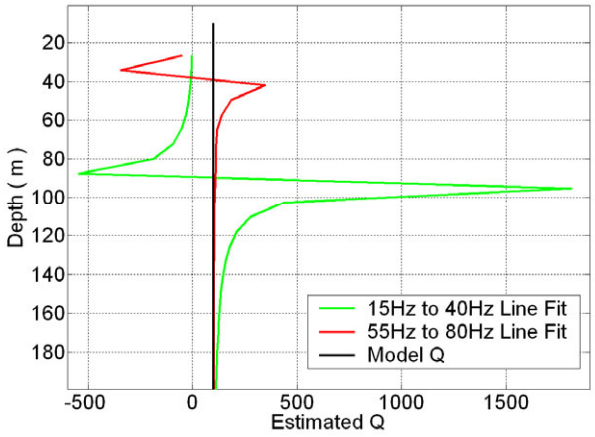

Figure 4: Apparent near-field frequency dependence of Q.

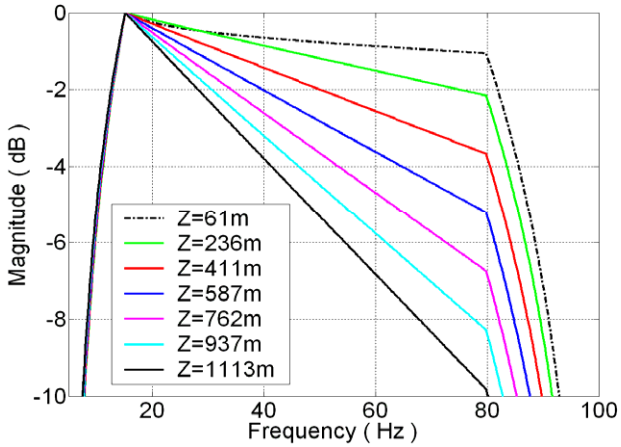

Figure 5: Far-field log-magnitude spectra (max. amp. equ.).

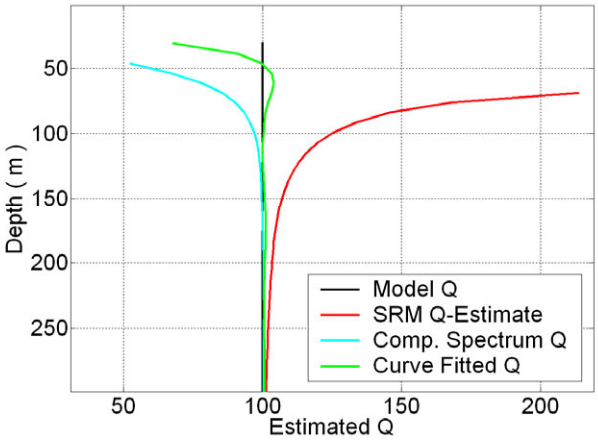

Figure 6: SRM Q-estimates with and without compensation.

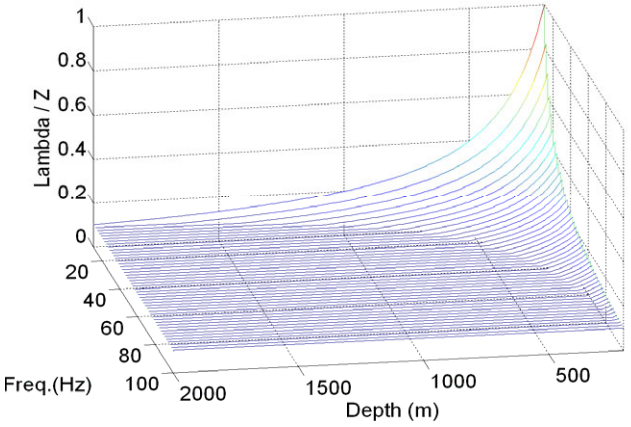

Figure 7: Relative near-field strength. Note the 10% cutoff.

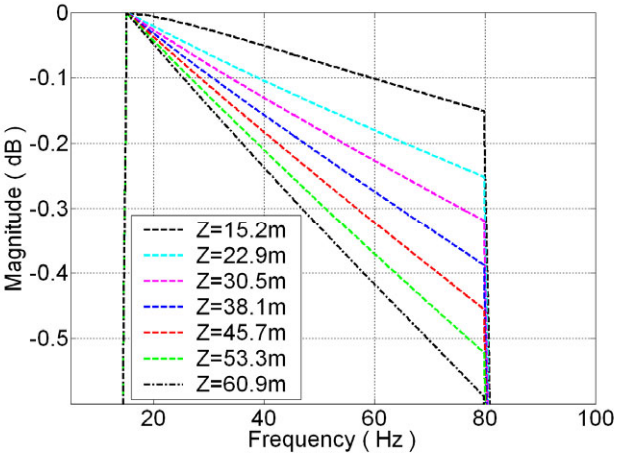

Figure 8: Near-field compensated log-magnitude spectra.